

## Gamma-ray Polarimetry \*

Hiroyasu Tajima

Stanford Linear Accelerator Center, Stanford University, Stanford, CA 94309

### Abstract

An astrophysics application of a low noise Double-sided Silicon Strip Detector (DSSD) is described. A Semiconductor Multiple-Compton Telescope (SMCT) is being developed to explore the gamma-ray universe in the 0.1–20 MeV energy band. Excellent energy resolution and polarization sensitivity are key features of the SMCT. We have developed prototype modules for a low noise DSSD system, which reached an energy resolution of 1.3 keV (FWHM) for 122 keV at 0°C. Results of a gamma-ray imaging test are also presented.

*Keywords: gamma-ray, Compton telescope, polarimeter, Silicon Strip Detector*

*Contributed to International Workshop on Vertex Detectors  
Kailua-Kona, Hawaii USA  
November 3–November 8, 2002*

---

\* This work was carried out in collaboration with T. Kamae and E. do Couto e Silva (SLAC), S. Uno, T. Nakamoto and Y. Fukazawa (Hiroshima University), T. Mitani, T. Takahashi and K. Nakazawa (Institute of Space and Astronautical Science) and D. Marlow (Princeton University), and supported by U.S. Department of Energy, contract DE-AC03-76SF00515, Grant-in-Aid by Ministry of Education, Culture, Sports, Science and Technology of Japan (12554006, 13304014), and “Ground-based Research Announcement for Space Utilization” promoted by Japan Space Forum.

## 1 Introduction

A low noise Double-sided Silicon Strip Detector (DSSD) is a fundamental element to realize a Semiconductor Multiple-Compton Telescope (SMCT)[1,2], which utilizes a multiple-Compton scattering technique to achieve good efficiency with high background rejection capability. The SMCT is a hybrid semiconductor gamma-ray detector, which consists of silicon and CdTe detectors. The excellent energy resolution of the SMCT allows it to detect photons with good angular resolution and background rejection capability. In addition, the ability to measure polarization, a wide energy band (0.1–20 MeV), a wide field of view ( $\sim 60^\circ$ ) and light weight are important properties of the SMCT. Polarization sensitivity enables us to study particle acceleration mechanisms in supernovae remnants, pulsars and black holes. Synchrotron radiation, inverse Compton scattering and bremsstrahlung are main photon processes and they produce distinct photon polarization features.

A stack of many thin scatterers is used in the multiple-Compton technique[3], which allows increased detection efficiency by stacking more elements, while maintaining the ability to record individual Compton scatterings.

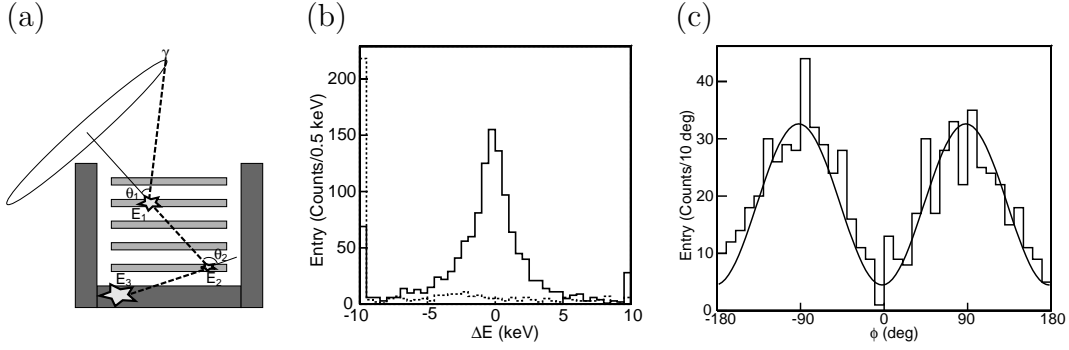


Fig. 1. (a) Concept of the Multiple-Compton technique. (b) Difference between calculated and measured electron recoil energy in EGS4 MC. Solid and dotted histograms indicate signal and backgrounds, respectively. (c) Reconstructed  $\phi$  distribution of the first Compton scatter in MC with 100% linear polarization.

Fig. 1 (a) illustrates the case with two Compton scatterings and one photo-electric absorption. In this situation, scattering angles  $\theta_1$  and  $\theta_2$  can both be obtained from the recoil electron energies as

$$\cos \theta_1 = 1 + \frac{m_e c^2}{E_1 + E_2 + E_3} - \frac{m_e c^2}{E_2 + E_3}, \quad \cos \theta_2 = 1 + \frac{m_e c^2}{E_2 + E_3} - \frac{m_e c^2}{E_3}, \quad (1)$$

where  $E_1$ ,  $E_2$  and  $E_3$  are the energy deposits in each photon interaction. Note that  $\theta_2$  can be reconstructed from the hit positions of the three interactions. The order of the interaction sequences, hence the correct energy and direction

of the incident photon, can be reconstructed by examination of this constraint for all possible sequences. This over-constraint also provides stringent suppression of random coincidence backgrounds. The direction of the incident photon can be confined in a cone determined from  $\theta_1$  and the first two interaction positions. Fig. 1 (b) shows a distribution of the difference of the recoil electron energy calculated from the scattering angle and the “measured” energy from a EGS4 Monte Carlo simulation[4] with low energy extension[5]. Solid and dotted histograms indicate signals and backgrounds, respectively. Underflows and overflows are shown in the leftmost and rightmost bins. The polarization of the incident photon can be measured by the azimuthal angle ( $\phi$ ) distribution of the first Compton scatter. Fig. 1 (c) shows the  $\phi$  distribution reconstructed from hits in DSSDs in a MC sample for 100 keV photons with 100% linear polarization. Clear modulation can be observed.

## 2 Low Noise SSD System

We have developed prototype modules for a low noise DSSD system in order to understand all noise sources in detail, which is necessary to achieve the best possible energy resolution. A low noise DSSD system consists of a DSSD, an RC chip and a VA32TA front-end VLSI chip[1,6]. To keep the strip yield close to 100%, the DSSD does not employ an integrated AC capacitor. We have produced 300  $\mu\text{m}$  thick DSSDs with strip lengths of 2.56 cm, strip gaps of 100  $\mu\text{m}$  and strip pitches of either 400  $\mu\text{m}$  or 800  $\mu\text{m}$ . The C-V curve measurement yields the depletion voltage of 65 V, therefore the following measurements are performed at 70 V bias. Leakage current is measured to be 0.5 nA/strip at 20°C and 0.05 nA/strip at 0°C. The strip capacitance is measured to be  $6.3 \pm 0.2$  pF for a 400  $\mu\text{m}$  pitch sample. A resistance value of 1 G $\Omega$  is chosen for bias resistor to minimize thermal noise without compromising production stability. Expected noise performance of VA32TA is  $(45 + 19 \times C_d)/\sqrt{\tau}$   $e^-$  (RMS) in ENC or  $(0.37 + 0.16 \times C_d)/\sqrt{\tau}$  keV (FWHM), where  $C_d$  is the detector load capacitance and  $\tau$  is the peaking time, which can be varied from 1 to 4  $\mu\text{s}$ .

We have assembled two prototype modules: one consists of a 400  $\mu\text{m}$  pitch SSD, an RC chip and a VA32TA (AC module); the other consists of an SSD and a VA32TA (DC module). Absolute gain of the system is calibrated using the  $\gamma$ -ray spectra obtained below. The DC module has yielded a best noise performance of 1.0 keV at 0°C and  $\tau = 4$   $\mu\text{s}$ , which is in a good agreement with the expected value derived from known noise performance of VA32TA and the measured strip capacitance.

The energy resolution for the  $\gamma$ -ray detection is investigated using the 59.54 keV  $\gamma$ -ray line from  $^{241}\text{Am}$  and the 122.06 keV  $\gamma$ -ray line from  $^{57}\text{Co}$ . Absolute gain

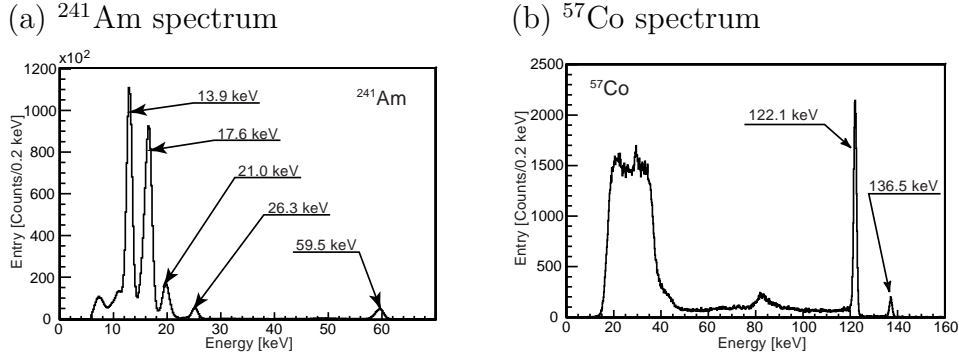


Fig. 2. Energy spectra of (a)  $^{241}\text{Am}$  and (b)  $^{57}\text{Co}$ .

is calibrated for each channel using the same  $\gamma$ -ray sources in such way that all channels give the nominal peak height. Figs. 2 (a) and (b) show the sum of the energy spectra for all channels, except for the first and last strips where we observe larger noise. We observe a clear Compton edge just below 40 keV in the  $^{57}\text{Co}$  spectrum. Note only 59.5 keV and 122.1 keV lines are calibrated. Energy resolution is measured to be 1.3 keV at  $0^\circ\text{C}$  and  $4\ \mu\text{s}$  for both 59.54 and 122.06 keV  $\gamma$ -rays. A detailed description of the SSD system and the noise and energy resolution measurements can be found elsewhere[1].

### 3 Imaging Test Results and Conclusions

In order to investigate the  $\gamma$ -ray imaging capabilities, we have assembled a DSSD module with an  $800\ \mu\text{m}$  pitch DSSD, RC chips and VA32TA ASICs. A  $^{57}\text{Co}$  source is placed 4 cm above the DSSD module. We select events in which one Compton scattering and one photoelectric absorption take place in a single DSSD as illustrated in Fig. 3 (a). Events with two hits on both sides and whose energy is greater than 10 keV are selected. Hits with larger energy deposits on both sides are paired to form a 2D hit. Remaining hits on both sides are paired to form another 2D hit. The energy difference of hits in each pair is required to be less than 7 keV to suppress wrong combinations. The pair of 2D hits must be separated by more than 0.4 cm to ensure adequate angular resolution for the scattered photon direction. The open histogram in Fig. 3 (b) shows the resulting distribution of the sum of average energies of two 2D hits. Fig. 3 (c) shows a  $\theta_{\text{kin}} - \theta_{\text{geo}}$  distribution for the events within 6 keV of the 122 keV peak, where  $\theta_{\text{kin}}$  is the Compton scattering angle calculated from two energy deposits using eq. (1) and  $\theta_{\text{geo}}$  is the angle calculated from the known source location and observed positions of the energy deposits. A fit to a sum of two Gaussian functions yields an angular resolution of  $13.4^\circ$  (FWHM), which is in a good agreement with the MC result of  $11.8^\circ$ . Dominant contributions are estimated to be Doppler broadening ( $8.8^\circ$ ), the energy resolution ( $6.0^\circ$ ) and

the angular resolution of scattered photon ( $5.1^\circ$ ). The latter two contributions can be reduced by using smaller strip pitch and removing RC chips. A hatched histogram in Fig. 3 (a) shows the energy sum distribution for the events with  $|\theta_{\text{kin}} - \theta_{\text{geo}}| < 12^\circ$ , which shows usefulness of such constraint. Fig. 3 (d) shows an image of the  $^{57}\text{Co}$  source produced by a superposition of all cones from the events within 6 keV of the 122 keV peak without a constraint on  $|\theta_{\text{kin}} - \theta_{\text{geo}}|$ .

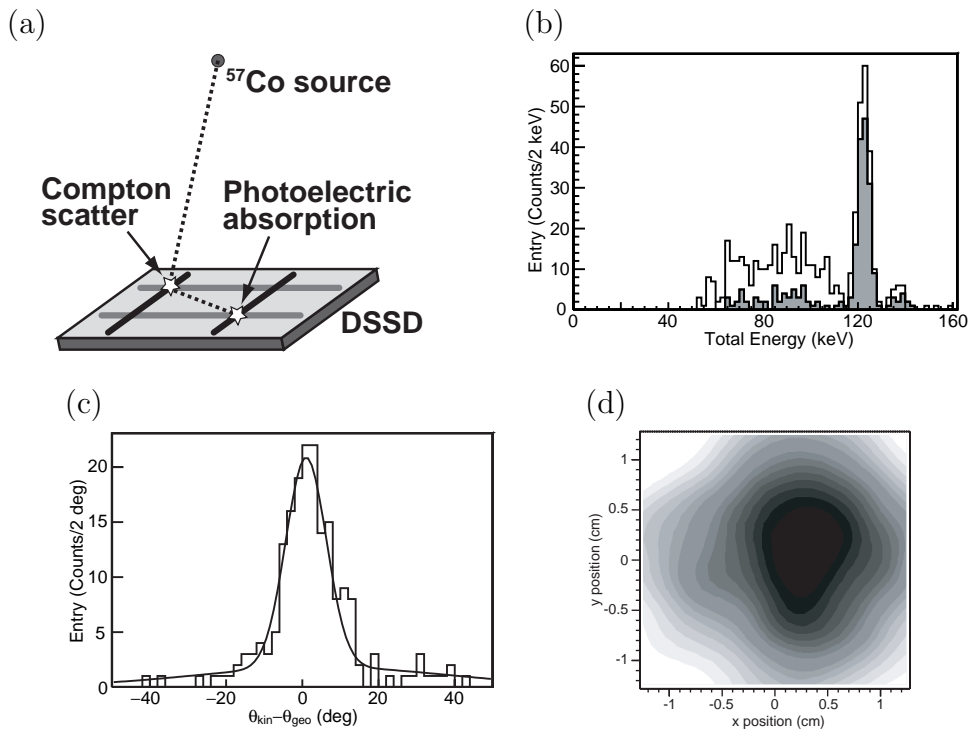


Fig. 3. (a) Illustration of one Compton scattering and one photo-absorption in a single DSSD. (b)  $^{57}\text{Co}$  spectrum with and without background suppression using source location constraints. (c)  $\theta_{\text{kin}} - \theta_{\text{geo}}$  distribution for the events within 6 keV of the 122 keV peak. (d)  $^{57}\text{Co}$ -source image reconstructed using Compton kinematics.

In conclusion, we have fabricated prototype modules for a DSSD system, which is a crucial element of the SCMT. Intrinsic noise performance is measured to be 1.0 keV (FWHM) at  $0^\circ\text{C}$  in the DC configuration, which is in good agreement with the analytically calculated noise value of 0.9 keV. The energy resolution is measured to be 1.3 keV (FWHM) in the same configuration, indicating that an energy resolution of 1 keV is within reach. Gamma-ray imaging with a DSSD using Compton kinematics is demonstrated for energy around 0.1 MeV.

## References

- [1] H. Tajima, et al., Low noise double-sided silicon strip detector for multiple-Compton gamma-ray telescope, in: J. E. Truemper, H. D. Tananbaum (Eds.), X-ray and Gamma-ray Telescopes and Instruments for Astronomy, SPIE, Vol. 4851, SLAC-PUB-9493, ISAS-RN-754, astro-ph/0212053, 2002.
- [2] T. Takahashi, et al., High resolution CdTe detectors for the next generation multi-Compton gamma-ray telescope, in: J. E. Truemper, H. D. Tananbaum (Eds.), X-ray and Gamma-ray Telescopes and Instruments for Astronomy, SPIE, Vol. 4851, 2002.
- [3] T. Kamae, R. Enomoto, N. Hanada, A new method to measure energy, direction, and polarization of gamma rays, Nucl. Inst. and Meth A 260 (1987) 254.
- [4] W. R. Nelson, H. Hirayama, D. W. O. Rogers, The EGS4 code system, SLAC-Report-265, 1985.
- [5] Y. Namito, S. Ban, H. Hirayama, Implementation of linearly-polarized photon scattering into the EGS4 code, Nucl. Inst. and Meth A 332 (1993) 277–283.
- [6] O. Toker, S. Masciocchi, E. Nygård, A. Rudge, P. Weilhammer, VIKING, a CMOS low noise monolithic 128 channel frontend for Si-strip detector readout, Nucl. Inst. and Meth A 340 (1994) 572–579.